Advances in Water Resources 195 (2025) 104858

Contents lists available at ScienceDirect

Advances in Water Resources

journal homepage: www.elsevier.com/locate/advwatres

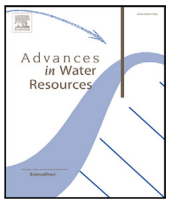

# In search of non-stationary dependence between estuarine river discharge and storm surge based on large-scale climate teleconnections

Georgios Boumis [a,b,*], Hamed R. Moftakhari [a,b], Danhyang Lee [c], Hamid Moradkhani [a,b]

[a] Center for Complex Hydrosystems Research, University of Alabama, Box 870205, Tuscaloosa, AL 35487-0205, USA
[b] Department of Civil, Construction, and Environmental Engineering, University of Alabama, Box 870205, Tuscaloosa, AL 35487-0205, USA
[c] Department of Statistical Science, Baylor University, Box 97140, Waco, TX 76798-7140, USA

## ARTICLE INFO

Dataset link: https://grdc.bafg.de/, https://gesla787883612.wordpress.com/, https://bmcnoldy.earth.miami.edu/tropics/oni/, https://climatedataguide.ucar.edu/climate-data/hurrell-north-atlantic-oscillation-nao-index-station-based/, https://github.com/bgeorgios/BDCop4CF

*Keywords:*
Estuarine environments
River discharge
Storm surge
Compound floods
Bivariate hazard
Dynamic copulas
Climate patterns
Bayesian statistics

## ABSTRACT

Compound floods may happen in low-lying estuarine environments when sea level above normal tide co-occurs with high river flow. Thus, comprehensive flood risk assessments for estuaries should not only account for the individual hazard arising from each environmental variable in isolation, but also for the case of bivariate hazard. Characterization of the dependence structure of the two flood drivers becomes then crucial, especially under climatic variability and change that may affect their relationship. In this article, we demonstrate our search for evidence of non-stationarity in the dependence between river discharge and storm surge along the East and Gulf coasts of the United States, driven by large-scale climate variability, particularly El-Niño Southern Oscillation and North Atlantic Oscillation (NAO). Leveraging prolonged overlapping observational records and copula theory, we recover parameters of both stationary and dynamic copulas using state-of-the-art Markov Chain Monte Carlo methods. Physics-informed copulas are developed by modeling the magnitude of dependence as a linear function of large-scale climate indices, i.e., Oceanic Niño Index or NAO index. After model comparison via suitable Bayesian metrics, we find no strong indication of such non-stationarity for most estuaries included in our analysis. However, when non-stationarity due to these climate modes cannot be neglected, this work highlights the importance of appropriately characterizing bivariate hazard under non-stationarity assumption. As an example, we find that during a strong El-Niño year, Galveston Bay, TX, is much more likely to experience a coincidence of abnormal sea level and elevated river stage.

## 1. Introduction

Coastal floods are widely considered to be among the most devastating catastrophes, since they happen at areas which have a dense population and high environmental, social and economic importance (Haigh and Nicholls, 2017). At estuaries, i.e., coastal areas where rivers meet the sea, floods may be a result of multiple hydro-meteorological factors that can act simultaneously, not necessarily driven from a single phenomenon which acts in isolation (Harrison et al., 2022). For example, in low-lying estuarine environments, like bays that receive freshwater inputs, so-called "compound" floods may happen due to a coincidence of an elevated river stage and an increased sea level from, e.g., heavy rainfall and strong winds, respectively (Moftakhari et al., 2017, 2019). While high river discharge can also be regulated by other factors such as rapid snowmelt or flood management operations, the simultaneous or closely timed occurrence of inland floodwaters and ocean surge are mainly assumed to be due to a tropical storm. Such events typically produce floodwaters that are longer in duration and more widespread, in comparison with purely fluvial or ocean-driven estuarine floods. This was the case, for example, with Hurricane Harvey (2017), which induced a catastrophic compound flood around Galveston Bay, TX, lasting several days, due to a near coincidence of high river discharge from both Buffalo Bayou and San Jacinto River and ocean-derived storm surge (Valle-Levinson et al., 2020; Huang et al., 2021).

The traditional approach to coastal flood risk assessment addresses flood hazard from each driver independently, i.e., employs univariate statistical modeling (Hawkes et al., 2008). This relies on the assumption of no significant interactions between coastal flood drivers. However, comprehensive flood risk management for estuarine systems requires consideration of a probable co-occurrence (or sequence) of flood mechanisms, e.g., river discharge and storm surge, as mentioned earlier. Hence, it necessitates multivariate statistical modeling (Wu et al., 2021). This becomes increasingly important considering the fact that current research suggests that compound coastal floods might become more frequent and/or more severe in the future, as a result of long-term shifts in storm patterns, e.g., (extra)tropical cyclones and/or

* Corresponding author.
*E-mail address:* gboumis@crimson.ua.edu (G. Boumis).

https://doi.org/10.1016/j.advwatres.2024.104858
Received 25 August 2024; Received in revised form 25 November 2024; Accepted 27 November 2024
Available online 3 December 2024

upland development, among other factors (Dykstra and Dzwonkowski, 2021; Sebastian, 2022; Jafarzadegan et al., 2023). An essential part of multivariate flood hazard modeling is the characterization of the dependence structure of the flood drivers involved (Zhang et al., 2022; Tripathy et al., 2024). In practice, this characterization consists of two crucial steps: (1) the evaluation of whether there exists a statistically significant dependence between the different variables involved, and (2) the construction of a multivariate probability distribution that properly models (i.e., "fits") the data. Once these two steps have been completed, multivariate hazard curves can be then obtained in order to provide information about the recurrence interval, also known as return period, of different multivariate hazard scenarios (Salvadori et al., 2011). Complications in multivariate hazard modeling arise when the dependence structure of the flood drivers does not remain unchanged, but rather exhibits non-stationarity. This can happen, for example, when the magnitude of dependence has been varying over time. Nevertheless, with regard to the two steps outlined above, it is a rather difficult task to provide statistically robust evidence that the magnitude of dependence has been changing over the years and to subsequently incorporate this change into the construction of the multivariate probability distribution.

To this day, only a handful of studies, conducted on a broad spatial scale, have explored the possibility of non-stationarity in the interplay among factors that contribute to compound floods. For example, Wahl et al. (2015) performed a robust statistical analysis utilizing prolonged observational records and a sliding time window to compute the magnitude of dependence between precipitation and storm surge along the United States (US) coastline and showed that their interaction has changed over the years. In a similar manner, Gori et al. (2022) made use of complex physics-based models to simulate historical and projected tropical cyclone climatology over the Northeast and South(east) US to conclude that bivariate flood hazard from precipitation and storm surge is expected to dramatically increase by the end of this century. Only recently, in a comprehensive observation-based study, Nasr et al. (2023) demonstrated historical shifts in the extremal dependence between river discharge, precipitation and storm surge, linking them to large-scale climate patterns.

There appears to be, in addition, a shortage of scientific literature concerning a realistic and physically meaningful modeling of the possibly varying dependence structure of compound flood drivers; the majority of studies published on the matter have let multivariate distributions co-vary with *time*, i.e., an abstract quantity not directly linked to the physical mechanisms that may drive compound floods. As an example, Razmi et al. (2022) employed a multivariate distribution to simultaneously model extreme sea level and precipitation in New York City, US, allowing for a time-dependent change in the magnitude of their correlation. In an analogous manner, Pirani and Najafi (2023) utilized time-varying multivariate distributions to model the dependence structure of fluvial, pluvial and oceanic drivers of compound floods along the Canadian coasts. Similarly, Wang et al. (2023) captured changes in the multivariate distribution of concurrent precipitation and storm surge in Ho Chi Minh City, Vietnam, by using time-dependent parameters of a multivariate distribution.

To the best of our knowledge, there has yet to be a study that combines an evaluation of varying interactions between compound flood drivers with a pragmatic approach to dependence structure modeling. For this reason, here we develop a parsimonious framework to simultaneously search for non-stationary dependence between co-occurring flood variables as well as model their multivariate distribution. Specifically, we leverage long overlapping records of river discharge and storm surge, originating from major estuaries along the East and Gulf coasts of the US, in order to obtain stationary and dynamic multivariate distributions using advanced Bayesian techniques. The use of pertinent large-scale climate indices for modeling dynamic conditions allows us to provide a physically meaningful interpretation of changes, if any, in the dependence magnitude, in contrast to the use of *time* as an abstract covariate. Lastly, Bayesian model intercomparison through appropriate metrics casts light on whether there is evidence for a non-stationary dependence. Along the way, we show how parametric uncertainty in the multivariate distribution can be reduced by formulating a meaningful and informative prior distribution, within the Bayesian context, that is based on the variability of observed dependence between river discharge and storm surge. Also, we highlight the implications of inappropriate bivariate hazard quantification under stationarity assumption for estuaries where the dependence indeed co-varies with large-scale climatic phenomena. The rest of this article is organized as follows: Section 2 describes the different data sources used and the statistical methods employed, concluding with a diagram which describes our overall methodological framework. Section 3 includes the results of our analysis along with discussions and interpretations of them, while our study is finalized in Section 4 where we outline methodological limitations of our work as well as suggestions for future research.

## 2. Datasets and methodology

### 2.1. River discharge and storm surge data

Average daily river discharge data were firstly downloaded from the Global Runoff Data Center (GRDC). We then quality-constrained the river discharge data from GRDC by keeping years of record with $> 80\%$ of non-missing entries. In addition, we downloaded hourly measurements of still water level (SWL) from tide stations along the East and Gulf coasts of the US, which are archived at the latest version of the GESLA database (Haigh et al., 2023). Next, to obtain the storm surge, which is essentially the only meteorological, and thus stochastic, component of SWL (Serafin et al., 2017), we conducted a tidal harmonic analysis. Specifically, we predicted the tidal level, including mean sea level (MSL), and subtracted it from SWL to extract the random non-tidal residual, or else, surge. The tidal harmonic analysis was carried out on an annual basis to discount the effect of MSL rise and involved 60 influential tidal constituents, analogous to the work of Boumis et al. (2024). Similar to discharge, the time series of hourly surge was quality-controlled by removing years for which $\geq 20\%$ of the data were missing. We made sure that the corresponding tide gauges are in close proximity to the respective estuaries where the river data pertain to ("great-circle" distance $< 250$ km), considering also the interconnectivity of sea levels. Finally, we matched the time resolution of the two datasets by extracting the maximum hourly surge per day and kept estuaries for which the overlapping observational record was longer than 50 years. The latter resulted in a total of ten river gauge and tide station combinations from nine estuaries distributed along the East and Gulf coasts of the US; these were used for further analyses. Table 1 summarizes information about the estuaries under study, including river gauge and tide station geographic location, as well as the "great-circle" distance (km) between them. At this point, it is worth mentioning that our study site selection, particularly in terms of river gauge location, does not account for upstream human operations which can modulate river discharge and thus can artificially influence dependence (refer to "Methodological limitations and conclusion").

### 2.2. Large-scale climate indices

To model a physics-informed varying magnitude of dependence (see Section 2.4), we utilized historic monthly Oceanic Niño Index (ONI) values that are hosted online from the University of Miami. ONI is a popular and widely used metric to identify the warm (or cool) anomaly of sea-surface temperature in the central-to-eastern equatorial Pacific Ocean with respect to historic normal conditions (Glantz and Ramirez, 2020). In other words, ONI is used to define the phase of El-Niño Southern Oscillation (ENSO) that is known to have teleconnections all around the globe, including the Southeast and Gulf coasts of the US which are under consideration in this study (Taschetto et al., 2020). For

**Table 1**
Geographical information of estuaries under study and approximate "great-circle" distance (km) between river gauges and respective tide stations.

| Estuary | River gauge | Longitude | Latitude | Tide station | Longitude | Latitude | Distance |
|---|---|---|---|---|---|---|---|
| Upper New York Bay | Hudson River | −73.69 | 42.75 | The Battery, NY | −74.01 | 40.70 | 230 |
| Merrimack Estuary | Merrimack River | −71.30 | 42.65 | Boston, MA | −71.05 | 42.36 | 38 |
| Upper Chesapeake Bay | Susquehanna River | −76.18 | 39.66 | Baltimore, MD | −76.58 | 39.27 | 55 |
| Lower Chesapeake Bay | Potomac River | −77.13 | 38.95 | Washington, D.C. | −77.02 | 38.78 | 21 |
| Winyah Bay | Pee Dee River | −79.55 | 34.20 | Charleston, SC | −79.92 | 32.78 | 162 |
| Tybee Roads Estuary | Savannah River | −81.27 | 32.53 | Fort Pulaski, GA | −80.90 | 32.04 | 65 |
| Tampa Bay | Alafia River | −82.21 | 27.87 | St. Petersburg, FL | −82.63 | 27.76 | 43 |
| Pensacola Bay | Escambia River | −87.23 | 30.97 | Pensacola, FL | −87.21 | 30.40 | 63 |
| Galveston Bay | Buffalo Bayou | −95.61 | 29.76 | Galveston Pier 21, TX | −97.79 | 29.31 | 217 |
| San Antonio Bay | Guadalupe River | −97.01 | 28.79 | Rockport, TX | −97.05 | 28.02 | 86 |

our application, we specifically obtained historic annual Oceanic Niño Indices by averaging monthly values. Additionally, we downloaded station-based yearly values of the North Atlantic Oscillation (NAO) index which are archived online at the National Center for Atmospheric Research. The NAO index, which is indicative of the difference in normalized sea-level pressure between Lisbon, Portugal, and Reykjavík, Iceland, is relevant for the under-study estuaries in the Northeast coasts of the US, as this climate phenomenon has been linked to intense weather systems over the North Atlantic (Hurrell et al., 2003; Hurrell and Deser, 2010).

### 2.3. Bivariate sampling and rank correlation coefficient

We followed a two-way conditional sampling approach in order to extract co-occurring discharge ($Q$) and surge ($S$) with at least one variable being extreme. Particularly, we extracted annual maxima of the first, i.e., conditioning variable and then the respective maximum value of the second, i.e., conditioned variable with a lag of +/- 1 to 10 days; we refer to pairs where surge is conditioned on discharge as $Q\_S$, while reversely we denote pairs where discharge is conditioned on surge as $S\_Q$. We chose to investigate long time lags, up to 10 days, as we did not correct for the travel time between the location where discharge is being measured and the outlet of the estuary where river flow meets sea water. This approach is in-line with earlier works that investigated bivariate dependence between river discharge and storm surge, e.g., Nasr et al. (2021). Besides, compound floods can have cumulative effects even when the events occur on different days but within a short time window; the latter event can affect recovery actions taken in response to the former event. Once the corresponding two-way conditional samples were collected, we then quantified the magnitude of dependence between river discharge and storm surge by computing the Kendall's $\tau$ rank correlation coefficient and its significance (Abdi, 2007). We opted for Kendall's $\tau$ instead of Pearson's linear correlation coefficient, because the former can capture a non-linear dependency as well. Lastly, we decided to work with either $Q\_S$ or $S\_Q$ pairs and the optimal time lag which altogether yielded the maximum statistically significant Kendall's $\tau$ rank coefficient.

### 2.4. Dependence structure modeling with Bayesian (dynamic) copulas

Characterizing the dependence structure of river discharge and storm surge means constructing a joint probability distribution for the two random variables $Q$ and $S$. To do so, we employed copula theory (Salvadori and De Michele, 2004, 2007; Durante and Sempi, 2010) which has been used in many different scientific fields, including the hydroclimatic domain (Tootoonchi et al., 2022). A copula ($C$) is a mathematical function that connects a bivariate distribution to the underlying cumulative marginals; its significant advantage is that it does so without any constraint on the family or form of the marginals (Czado, 2019). According to Sklar's theorem (Sklar, 1959), the bivariate distribution $F_{QS}$ with marginals $F_Q$ and $F_S$ can be written as:

$$C(u,v) = F_{QS}(F_Q^{-1}(u), F_S^{-1}(v)) \tag{1}$$

where $C \in [0,1]^2$ is a 2-dimensional copula, which in the case of absolutely continuous distributions is unique. Here, $u$ and $v$ are transformed variables of river discharge ($Q$) and storm surge ($S$), such that $u = F_Q(q)$ and $v = F_S(s)$, respectively. An empirical copula approximation can be defined as:

$$\tilde{C}(u,v) = \frac{1}{n+1}\sum_{i=1}^{n} I_{\{u_i \le u, v_i \le v\}} \tag{2}$$

with $u$ and $v$ expressed as:

$$u = \tilde{F}_Q(q) = \frac{1}{n+1}\sum_{i=1}^{n} I_{\{q_i \le q\}} \tag{3}$$

$$v = \tilde{F}_S(s) = \frac{1}{n+1}\sum_{i=1}^{n} I_{\{s_i \le s\}} \tag{4}$$

where $\{(q_i, s_i) : i = 1, \ldots, n\}$ is the bivariate sample of size $n$ and $I(\cdot)$ is an indicator function.

The empirical copula modulates the choice of a suitable theoretical, or else, parametric copula. There are various theoretical copulas, each with distinct characteristics, that can capture the structure and strength of dependence between two random variables (Vogl et al., 2012). The most widely used families of theoretical copulas are the so-called "Archimedean" and "Elliptical" copulas (Tootoonchi et al., 2020). For our analysis, we chose to work with three popular Archimedean copulas, i.e., Frank, Gumbel and Clayton, which all together can be used to assess different dependence structures where the strength of dependence might (or might not) be concentrated either in the upper or lower tail (refer to next paragraph). These copulas, in contrast to Elliptical, have closed-form expressions, their parameter can be directly connected to Kendall's $\tau$ (see below) and are easier to sample from. Specifically, the bivariate Frank copula function is given by:

$$\underset{\text{Frank}}{C}(u,v) = -\frac{1}{\delta}\log\left(\frac{1}{1-e^{-\delta}}[(1-e^{-\delta}) - (1-e^{-\delta * u})(1-e^{-\delta * v})]\right) \tag{5}$$

where the copula parameter $\delta \in (-\infty, \infty)\backslash\{0\}$, and as $\delta \to 0^+$, it leads to the independence copula. Note that there exists a closed-form equation that directly links Kendall's $\tau$ with $\delta$ (Frees and Valdez, 1998):

$$\tau = 1 - \frac{4}{\delta} + 4 * \frac{D_1(\delta)}{\delta} \tag{6}$$

where $D_1(\delta)$ is the first-order Debye function expressed as follows:

$$D_1(\delta) = \int_0^{\delta} \frac{x/\delta}{e^x - 1} dx. \tag{7}$$

The other two bivariate copula functions, i.e., Gumbel and Clayton, are provided in Text S1.

For each bivariate sample, we performed a goodness-of-fit test to assess whether the dependence structure could be parameterized by a Frank copula, which constitutes the null hypothesis. This was done by computing the test statistic $S_n$ as described in Genest et al. (2009), with its $p$-value obtained using a parametric bootstrap approach with $N = 500$ bootstrap replications. The rationale behind undertaking this test as a first step of bivariate modeling is that the Frank copula is symmetric and does not exhibit tail dependence, which makes it suitable for modeling variables where joint occurrences of extreme values (either high or low) are not more probable than joint occurrences

of moderate values. Conversely, the Gumbel copula is asymmetric and exhibits upper tail dependence, making it suitable for modeling variables where joint occurrences of high values are more probable than joint occurrences of moderate or low values. Similarly, the Clayton copula is asymmetric and exhibits lower tail dependence, making it suitable for modeling variables where joint occurrences of low values are more probable than joint occurrences of moderate or high values. Thus, the Frank copula's lack of tail dependence makes it a good initial choice for modeling balanced bivariate dependence structures, where extreme joint occurrences are not expected to be biased towards either tail. Besides, the unconstrained support of Frank copula's parameter ($\delta \in R \setminus \{0\}$), allows us to construct informative prior distributions in the context of Bayesian analysis more easily (see Section 3.3). In cases where we rejected the null hypothesis, we instead performed the goodness-of-fit test using the Gumbel and Clayton copulas to decide which of the two functions is more suitable for modeling the dependence structure.

Once a suitable copula function was selected for each bivariate sample, we next retrieved the model parameter ($\delta$), indicative of the magnitude of dependence, for both a stationary copula and a dynamic copula. Specifically, we modeled a physics-informed copula by allowing the parameter $\delta$ to linearly co-vary with a large-scale climatic pattern ($Climate\_Index$) as follows:

$$\delta = b + w * Climate\_Index \tag{8}$$

where $b$ is the bias term and $w$ is the weight term, while $Climate\_Index$ can be either ONI or NAO index in this analysis. It is important to note again here that we search for non-stationarity induced only by these particular climate modes. This variable, i.e., $Climate\_Index$ could in general be selected based on the hypothesized driver of non-stationarity and so the framework is flexible to be implemented under other teleconnections which might be more relevant for other coastal regions. Copula parameters in this analysis were recovered by means of Bayesian inference to properly quantify parametric uncertainty and facilitate its reduction via prior distribution analysis (refer to Section 3.3). In particular, for the case of a stationary copula, the Bayes' rule can be applied to express the posterior distribution of $\delta$ given $u$ and $v$ as follows:

$$\underbrace{p(\delta|u,v)}_{\text{posterior}} \propto \underbrace{c(u,v|\delta)}_{\text{likelihood}} \underbrace{p(\delta)}_{\text{prior}} \tag{9}$$

where $c(u,v) = \frac{\partial^2 C(u,v)}{\partial u \partial v}$ denotes the copula density function. Similarly, when modeling a physics-informed copula, the posterior distribution of $(b,w)$ given $u$ and $v$ is:

$$\underbrace{p(b,w|u,v)}_{\text{posterior}} \propto \underbrace{c(u,v|b,w)}_{\text{likelihood}} \underbrace{p(b,w)}_{\text{prior}}. \tag{10}$$

For stationary copulas, we initially chose $p(\delta)$ to be a completely uninformative improper prior, i.e., $U(-\infty,\infty)$, $U[1,\infty)$, or $U(0,\infty)$, for Frank, Gumbel, and Clayton, respectively. Similarly, for dynamic copulas, we selected $U(-\infty,\infty)$ as a prior distribution for both $b$ and $w$, assuming $p(b,w) = p(b)p(w)$, rejecting samples which led to $\delta < 1$ or $\delta \leq 0$ for Gumbel and Clayton, respectively (see text S1). The rationale behind these uninformative flat priors is that we generally do not know how $\delta$ is distributed. Besides, such priors exempt us from performing a prior sensitivity analysis. Because the left hand-side expression in both Eqs. (9) & (10) does not admit to a closed-form known probability density function, we approximated the posterior distribution utilizing Hamiltonian Monte Carlo (HMC) (Betancourt, 2017; Thomas and Tu, 2021), which is an advanced variant of Markov Chain Monte Carlo (MCMC). We employed four parallel HMC chains each initialized at a different start point. The total number of iterations was $M = 4 \times 4,000 = 16,000$, with half of them considered as warm-up phase. We then assessed convergence to the target density by computing two widely used metrics, namely, the split-$\hat{R}$ and the effective sample size ($n_{eff}$) (Vehtari et al., 2021), as well as by visual inspection of trace plots. Bayesian inference was done with the use of Stan (Gelman et al., 2015) and its R interface, i.e., *rstan*.

### 2.5. Bayesian model comparison

To facilitate comparison between stationary and dynamic copulas within the Bayesian context, we then employed two metrics which are particularly suitable when different models have been obtained via MCMC simulation. Specifically, we computed both the Deviance Information Criterion (DIC) (Spiegelhalter et al., 2002) and the Widely Applicable Information Criterion (WAIC) (Watanabe and Opper, 2010). The first metric is given by the following expression:

$$DIC = -2 * \log[c(u,v|\hat{\theta}_{Bayes})] + 2 * p_{DIC} \tag{11}$$

$$p_{DIC} = 2 * (\log[c(u,v|\hat{\theta}_{Bayes})] - \frac{1}{K}\sum_{k=1}^{K} \log[c(u,v|\theta^k)]) \tag{12}$$

where $\theta$ denotes the parameter(s) of the model, i.e., $\delta$ or $(b,w)$, for stationary and dynamic copulas, respectively, while $c(u,v|\theta)$ is the joint predictive copula density evaluated at $\theta$. $\hat{\theta}_{Bayes}$ is the posterior mean(s), $\theta^k$ is the $k$th sample from the posterior distribution via HMC, and $K$ is the total number of post-warm-up MCMC iterations, i.e., $K = M - 8000 = 8000$. The formula for the second metric is shown below:

$$WAIC = -2 * \sum_{i=1}^{n} \log[\frac{1}{K}\sum_{k=1}^{K} c(u_i,v_i|\theta^k)] + 2 * p_{WAIC} \tag{13}$$

$$p_{WAIC} = 2 * \sum_{i=1}^{n} (\log[\frac{1}{K}\sum_{k=1}^{K} c(u_i,v_i|\theta^k)] - \frac{1}{K}\sum_{k=1}^{K} \log[c(u_i,v_i|\theta^k)]) \tag{14}$$

Both metrics, DIC and WAIC, provide a measure of within-sample predictive accuracy. However, the latter can also be viewed as an approximation to leave-one-out cross-validation since it averages over the entire posterior distribution (see Eqs. (13)–(14)) instead of relying on a point estimate, i.e., $\hat{\theta}_{Bayes}$, like the former (refer to Eqs. (11)–(12)) (Gelman et al., 2014). Models with lower DIC and WAIC values should be generally preferred over models whose corresponding metrics are greater. The entire methodological procedure (i.e., Sections 2.1 to 2.5) is summarized as a diagram shown in Fig. 1. Note that the "No" path in the first orange ellipsis encompasses also the case where a statistically significant negative correlation is detected. In this situation, rather than using multivariate modeling to account for the negative bivariate dependence, we recommend opting for univariate modeling. This more conservative approach helps to avoid underestimating the hazard that may result from either flood driver individually, which is important for engineering applications such as construction of either fluvial or coastal flood defenses.

## 3. Results and discussion

### 3.1. Dependence between river discharge and storm surge

Table 2 shows the maximum Kendall's $\tau$, the respective type of pairs ($Q\_S$ or $S\_Q$) and the optimal time lag for each estuary of our analysis; the number of pairs is also shown for reference. For most estuaries, rank correlation coefficients were found to be rather low, i.e., $\leq 0.24$, while the optimal time lag was quite short, i.e., 1 or 2 days. Higher coefficients were obtained for Upper Chesapeake Bay and Tampa Bay, i.e., 0.33 and 0.31, respectively, while Lower Chesapeake Bay displayed the greatest Kendall's $\tau$ with a value of 0.67. This might be partially due to the fact the Potomac River's flux into Chesapeake Bay is significantly influenced by the downstream boundary dominated by tidal processes. However, all rank correlation coefficients were found to be significantly different than zero at the 90% confidence level (Table 2). This finding suggests that there is indeed a statistically significant positive dependence between river discharge ($Q$) and storm surge ($S$) for the estuaries under study. On the contrary, the reverse type of pairs for most estuaries showed a statistically insignificant correlation at the 90% confidence level (see Table S1).

The Frank copula appeared to be an adequate mathematical function that can model the dependence structure of variables $Q$ and $S$

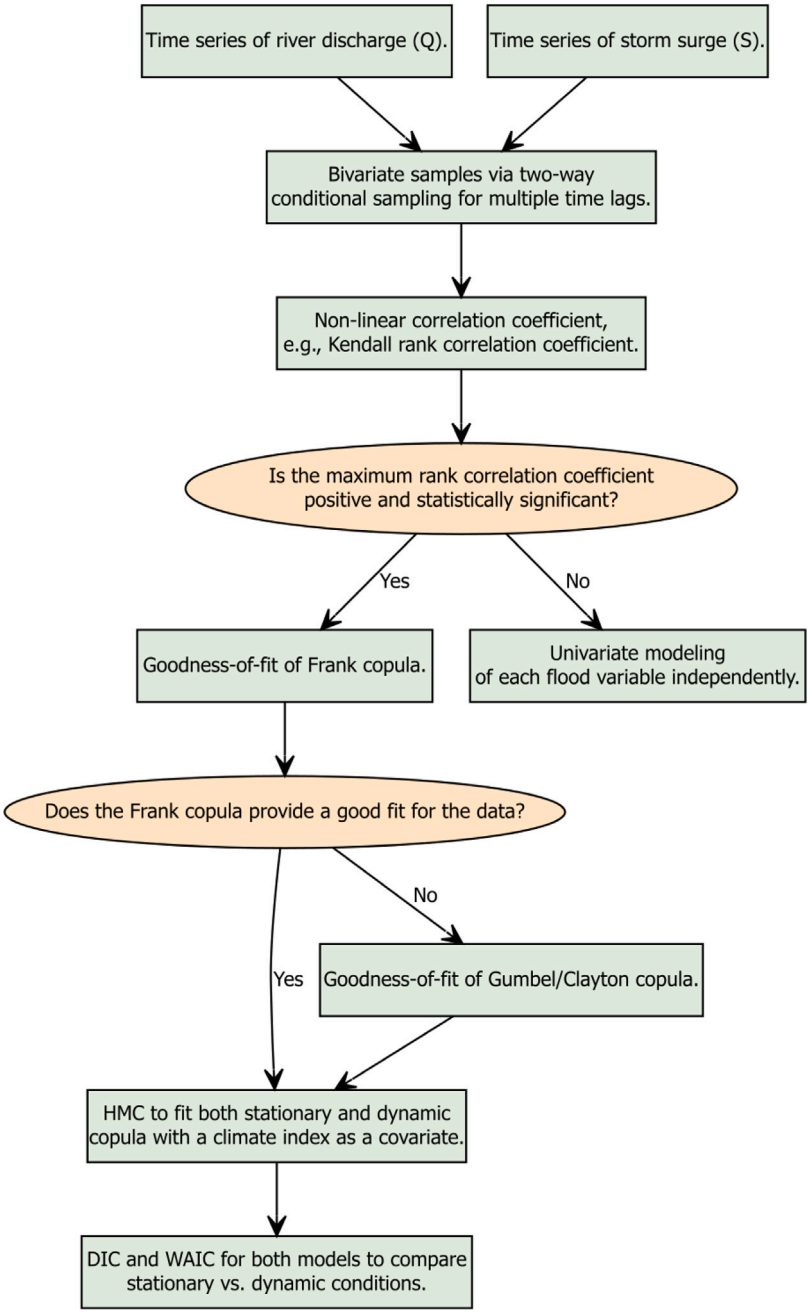


**Fig. 1.** Diagram of the methodological procedure to check for and model non-stationarity in the dependence structure of compound flood drivers.

for almost all estuaries. Specifically, based on the $S_n$ test statistic (Table 2), we failed to reject the null hypothesis that the bivariate data originate from a Frank copula ($\alpha = 0.10$), for all but one estuary. In particular, for Lower Chesapeake Bay, we derived a very small $p$-value ($<0.05$) suggesting that the Frank copula does not provide a good fit; on the contrary, for the same estuary, we failed to reject a Gumbel copula. These results should not come as a surprise since they are in accordance with a mere visual inspection of the bivariate data in the pseudo-observation domain (Figures S1 and S2). The scattered pairs of $u$ and $v$, observed for most estuaries under study, indicate an overall low positive dependence not concentrated at either tail, as opposed to Lower Chesapeake Bay where it is obvious that the dependence between $Q$ and $S$ is more pronounced at the upper tail (see top right panel in Figure S1).

Conclusively, here we argue that when dependence is indeed detected, the employment of a Frank copula is often a pragmatic and sufficient choice for modeling the dependence structure of co-occurring river discharge and storm surge, as demonstrated earlier. Most of the time, the characteristics (physical, morphological, etc.) of estuarine systems, in conjunction with a relatively short observational record, do not allow for strong upper- or lower-tail dependence to be detected, as it is the case with Lower Chesapeake Bay.

### 3.2. (Non-)stationarity of dependence between river discharge and storm surge

After running HMC for both stationary and dynamic copulas we obtained $n_{eff}$ values of $>$ 2000 and split-$\hat{R}$ values of $\sim$ 1 meaning

**Table 2**
Type (*Q_S* or *S_Q*) and number of pairs along with the optimal time lag (days) which resulted to the maximum rank correlation coefficient (Kendall's $\tau$) for each estuary under study. The statistical significance ($p$-value) of the Kendall's $\tau$ and the $S_n$ test statistic (Frank copula) is also shown.

| Estuary | Pairs | # Pairs | Time lag (days) | Kendall's $\tau$ | $P$-value (Kendall's $\tau$) | $P$-value ($S_n$) |
|---|---|---|---|---|---|---|
| Upper New York Bay | *Q_S* | 68 | 2 | 0.19 | <0.05 | >0.10 |
| Merrimack Estuary | *Q_S* | 97 | 1 | 0.24 | <0.05 | >0.10 |
| Upper Chesapeake Bay | *Q_S* | 52 | 1 | 0.33 | <0.05 | >0.10 |
| Lower Chesapeake Bay | *Q_S* | 87 | 1 | 0.67 | <0.05 | <0.05 |
| Winyah Bay | *S_Q* | 80 | 8 | 0.14 | <0.10 | >0.10 |
| Tybee Roads Estuary | *S_Q* | 78 | 4 | 0.14 | <0.10 | >0.10 |
| Tampa Bay | *S_Q* | 71 | 2 | 0.31 | <0.05 | >0.10 |
| Pensacola Bay | *Q_S* | 82 | 1 | 0.24 | <0.05 | >0.10 |
| Galveston Bay | *Q_S* | 68 | 2 | 0.19 | <0.05 | >0.10 |
| San Antonio Bay | *S_Q* | 59 | 1 | 0.19 | <0.05 | >0.10 |

**Table 3**
Deviance Information Criterion (DIC) and Widely Applicable Information Criterion (WAIC) as computed for both stationary and dynamic models. Posterior means and 90% credible intervals of parameters $\delta$ (stationary copula), $b$ and $w$ (dynamic copula) are also shown. Estuaries with an asterisk indicate cases where a dynamic copula is preferred over a stationary, based on both DIC and WAIC metrics.

| Estuary | $\text{WAIC}_{\text{stationary}}$ | $\text{DIC}_{\text{stationary}}$ | $\delta$ | $\text{WAIC}_{\text{dynamic}}$ | $\text{DIC}_{\text{dynamic}}$ | $w$ | $b$ |
|---|---|---|---|---|---|---|---|
| Upper New York Bay | −3.10 | −3.13 | 1.75 (0.47, 3.03) | −1.10 | −1.14 | 0.03 (−0.60, 0.71) | 1.72 (0.41, 3.07) |
| Merrimack Estuary | −10.30 | −10.16 | 2.17 (1.12, 3.23) | −8.70 | −8.49 | 0.16 (−0.38, 0.69) | 2.23 (1.18, 3.30) |
| Upper Chesapeake Bay* | −11.30 | −11.44 | 3.44 (1.86, 5.06) | −13.30 | −12.91 | 0.73 (0.07, 1.42) | 3.54 (2.09, 5.10) |
| Lower Chesapeake Bay | −128.50 | −128.30 | 3.18 (2.73, 3.66) | −126.90 | −126.46 | −0.05 (−0.27, 0.18) | 3.21 (2.76, 3.70) |
| Winyah Bay* | −1.10 | −1.15 | 1.25 (0.08, 2.38) | −1.80 | −2.17 | 2.14 (0.08, 4.14) | 1.27 (0.14, 2.40) |
| Tybee Roads Estuary | −1.70 | −1.43 | 1.30 (0.16, 2.44) | −1.10 | −0.69 | −1.42 (−3.44, 0.55) | 1.29 (0.11, 2.46) |
| Tampa Bay | −13.80 | −13.89 | 3.10 (1.81, 4.42) | −12.00 | −12.25 | 0.92 (−1.68, 3.69) | 3.01 (1.68, 4.32) |
| Pensacola Bay | −8.20 | −8.69 | 2.42 (1.20, 3.70) | −5.60 | −7.18 | −0.86 (−3.01, 1.21) | 2.40 (1.16, 3.63) |
| Galveston Bay* | −2.70 | −2.89 | 1.74 (0.44, 3.05) | −6.80 | −7.38 | 3.78 (1.31, 6.32) | 1.90 (0.56, 3.27) |
| San Antonio Bay | −2.10 | −2.08 | 1.70 (0.32, 3.10) | −0.60 | −1.68 | 1.69 (−0.42, 3.95) | 1.79 (0.36, 3.18) |

that the algorithm successfully converged to the target densities. For reference, the climate index used as a linear covariate for parameter $\delta$, i.e., used for modeling a physics-informed copula (Eq. (8)), is given in Table S2 for each estuary of our analysis. Table 3 displays mean parameter ($\delta$, $b$ and $w$) estimates along with their uncertainty, which is expressed here as 90% credible intervals; DIC and WAIC metrics are also presented in the same table for both models, i.e., stationary and dynamic. Our results revealed that a physics-informed copula, as modeled with ONI and NAO index covariates, provides a better model for only 3/10 estuaries under study. On the contrary, a stationary parameter $\delta$ yielded a more suitable fit for most estuaries. Notably, there is an agreement among DIC and WAIC metrics that a dynamic copula is more appropriate for capturing the dependence structure of estuarine river discharge and storm surge at Galveston Bay, Upper Chesapeake Bay and Winyah Bay, only. The same finding is also evident by examining the posterior distribution of parameter $w$, a distribution which summarizes the effect of the corresponding climate index on the magnitude of dependence. Specifically, for cases where the stationary copula was deemed more suitable, the posterior of $w$ spanned regions of both positive and negative samples, hence encompassing zero (see Table 3). In practice, this means that there is no clear indication as per what the effect of the covariate is (it can be either positive or negative), while there is also the chance of it being negligible, i.e., zero. Oppositely, for estuaries where a dynamic copula provided a superior fit, the credible intervals of parameter $w$ covered regions of positive samples, only (refer to Table 3), suggesting that a greater value of the respective climate index leads to a stronger dependence. Overall, our analysis indicated that there is no strong evidence for non-stationarity in the dependence between co-occurring river discharge and storm surge along the majority of the estuaries examined, particularly due to ENSO or NAO. It is important to note, however, that this finding is subject to the type of bivariate data employed and the choice of covariate (Table S2) used for capturing and modeling non-stationarity (see discussions on methodological limitations in Section 4).

### 3.3. Uncertainty of stationary copula parameter and Kendall's $\tau$-informed prior distribution

Given now that a stationary Frank copula can be used to properly model the dependence structure of river discharge and storm surge for most estuaries, as we showed earlier, it seems tempting to investigate possible ways for reducing estimation uncertainty and narrowing down credible intervals of parameter $\delta$ (Table 3). In fact, this type of parametric uncertainty is a major source of ambiguity in bivariate hazard curves, and consequently in bivariate hazard scenarios, which are critical for coastal flood risk assessments. Thus, efforts to minimize the uncertainty surrounding $\delta$ are very important. This is particularly useful for estuaries with a smaller number of bivariate pairs, which are consequently expected to exhibit higher uncertainty in the copula parameter.

Here we showcase a way to narrow down credible intervals of parameter $\delta$ by employing a rational Kendall's $\tau$-informed prior distribution instead of the typical $U(-\infty, \infty)$. For demonstration purposes, we choose to focus on San Antonio Bay which has a very small bivariate sample size of $n = 59$ "*S_Q*" pairs (Table 2). For this estuary, we found the mean value of parameter $\delta$ to be 1.70, while its 90% credible interval was (0.32, 3.10) (Table 3), based on the uninformative uniform prior. To derive a new meaningful and informative prior instead, we first bootstrapped bivariate samples with replacement for 1000 replications, keeping the sample size same as the original, i.e., $n = 59$. For each replication, we then computed a respective Kendall's $\tau$ and utilizing Eq. (6) we derived a corresponding $\delta$ parameter. This eventually led to a total of 1000 samples of parameter $\delta$, which we finally used in order to fit a distribution with Maximum Likelihood Estimation (MLE). Fig. 2 shows the histogram of these samples as well as a MLE-derived normal probability density that has an estimated mean of $\mu = 1.76$ and a standard deviation of $\sigma = 0.90$. This distribution, i.e., Normal(1.76, 0.90), constitutes a Kendall's $\tau$-informed prior for parameter $\delta$ that naturally reflects the expected variability in observed dependence between river discharge and storm surge at San Antonio Bay. After Bayesian inference with the new prior distribution, we obtained a mean parameter estimate of $\delta = 1.73$, which is very close

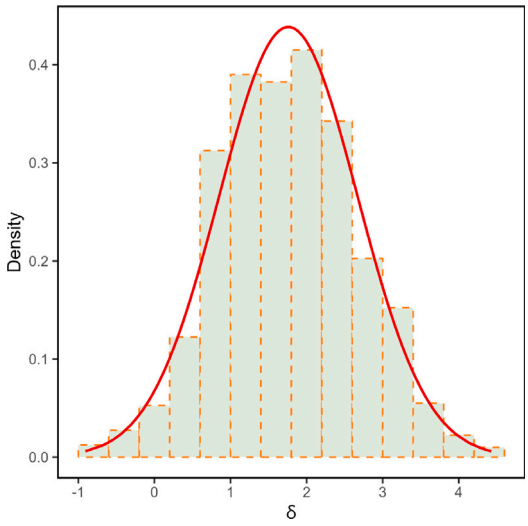


**Fig. 2.** Histogram of $\delta$ samples derived using Eq. (6) after bootstrap analysis of Kendall's $\tau$ for San Antonio Bay (light green bars with orange dashed lines). A normal probability density obtained via Maximum Likelihood Estimation is also shown (red solid line).

to the mean estimate using $U(-\infty, \infty)$ as a prior distribution. However, the 90% credible interval was narrowed down to (0.73, 2.74). This finding highlights the fact that deriving a Kendall's $\tau$-informed prior, as outlined here, can successfully reduce copula parametric uncertainty, even for cases where the bivariate sample size is relatively small. This smaller uncertainty is crucial from a practical point of view, as explained earlier.

### 3.4. Implications of non-stationarity for bivariate hazard scenarios

In occasions where a dynamic copula fits the data better, it is worth exploring what are the implications of inappropriate bivariate hazard quantification under an assumption of stationarity. For this reason, here we turn our focus on Galveston Bay, where both DIC and WAIC metrics clearly suggested that a dynamic copula whose parameter $\delta$ co-varies with ONI provides a superior fit than a stationary copula (Table 3). Specifically, for this estuary, we constructed and contrasted bivariate hazard curves based on both a stationary Frank copula with $\delta = 1.74$ and a dynamic copula with $w = 3.78$ and $b = 1.90$ (Table 3). The dynamic copula was based on a strong El-Niño year (ONI = 1.45), similar to the year 2015 CE. For the construction of smooth curves, as opposed to empirical, marginal distributions were fitted to both variables $Q$ and $S$ originating from the empirical bivariate sample. Particularly, since the bivariate sample for that estuary was of type "$Q\_S$", we employed a Generalized Extreme Value (GEV) distribution for river discharge and an Asymmetric Laplace (AL) distribution for surge. The cumulative probability functions for both GEV and AL distributions are shown in Text S2. The latter distribution was preferred for modeling surge, instead of a typical Gamma distribution, due to the fact that when $S$ is not the conditioning variable, it is possible to observe a negative surge for a combination of annual maximum discharge and the respective maximum surge within +/- 1 to 10 days. Both distributions were obtained by means of MLE and they provided a good fit to the respective empirical data (see Figures S3 and S4). Fig. 3 displays our bivariate hazard curves, both dynamic and stationary, with the red arrow highlighting an observed compound event which had $Q = 125$ m$^3$/s and $S = 0.60$ m. It is shown here that this compound event has a bivariate return period ("AND" scenario, see Salvadori et al. (2016) for definition of bivariate return periods) of roughly $T = 25$ years during a strong El-Niño year (left panel), but the exact same event has an approximate return period of $T = 80$ years under stationarity assumption (right panel). For estuaries where there is evidence for non-stationarity in the dependence structure of river discharge and storm surge, our analysis highlights the fact that stationary bivariate hazard curves could severely underestimate the likelihood of an event which can potentially lead to compound flooding, highly dependent on the year. In general, for cases where we found that a dynamic copula is more suitable, it appears that the likelihood of compound events gets higher with increasing signals of the respective large-scale climate pattern; see, e.g., the positive effects (i.e., posterior of $w$) of ONI or NAO index at Galveston Bay, Upper Chesapeake Bay and Winyah Bay (Table 3).

## 4. Methodological limitations and conclusion

In this work, we have searched for evidence of a varying dependence between estuarine river discharge and storm surge across the East and Gulf coasts of the US, driven by large-scale climate variability as expressed by ENSO and NAO. To this end, we developed a framework employing widely used Archimedean copulas, a goodness-of-fit test, state-of-the-art algorithms for Bayesian inference and informative Bayesian model comparison metrics, and we showed that for most estuaries examined here there is no strong indication of such non-stationarity. As part of our analysis, we also showed that, in practice, most of the time a Frank copula can sufficiently capture the dependence structure of river discharge and storm surge. In addition, we illustrated a useful way to reduce parametric uncertainty by employing a Kendall's $\tau$-informed prior distribution for the Frank copula parameter. Finally, through construction of bivariate hazard curves, we discussed the implications of ignoring non-stationarity when our framework suggests otherwise, concluding that during years where the signal from ENSO or NAO is strong, there is a higher chance of events that may cause compound flooding at certain estuaries. Our analysis does come, nevertheless, with limitations which we also discuss in the next paragraphs.

First, even though we have utilized lengthy available observational records of river discharge and storm surge, the overlapping time period is still considered rather short for us to extract many compound events where *both* variables, $Q$ and $S$, are considered extremes. This has limited our analysis to either pairs $Q\_S$ or $S\_Q$ (as described in Section 2.3). As a result, these data comprise a mixture of pairs, which, however, do include instances were both river discharge and storm surge are quite high (see bivariate data in Fig. 3 as an example). Consequently, our findings of (non-)stationarity in the dependence between river discharge and storm surge are representative of events which have *potential* to cause a compound flood, not of actual compound flood events. Besides, as mentioned earlier, very high river discharge measurements might as well be an artifact of upstream water management operations, not a direct influence of climate variability, and therefore may falsify the inference on natural dependence between the two variables. These limitations could possibly be alleviated by the use of prolonged continuous modeled river discharge and storm surge data, instead of observations. The rationale behind this is that with longer overlapping time series' of these variables it might be possible to obtain an adequate bivariate sample size where *both* $Q$ and $S$ are always extremes, i.e., not obtained from a two-way conditional sampling. In addition, most current modeled data typically reflect natural river discharge not affected by human operations, e.g., dam control. In such a case, any inference on (non-)stationary dependence would be more closely linked to *actual* compound flood drivers. The simulated data sets, however, should preferably originate from consistent models that are able to preserve the dependence between river discharge and storm surge. An idea for future research to this regard would be to utilize reanalysis river discharge data derived from ERA5 forcings, i.e., GloFAS-ERA5 (Harrigan et al., 2020) in conjunction with a newly developed hindcast model of storm surge that also utilizes ERA5 forcings (Mentaschi et al., 2023). Ideally, these models should however

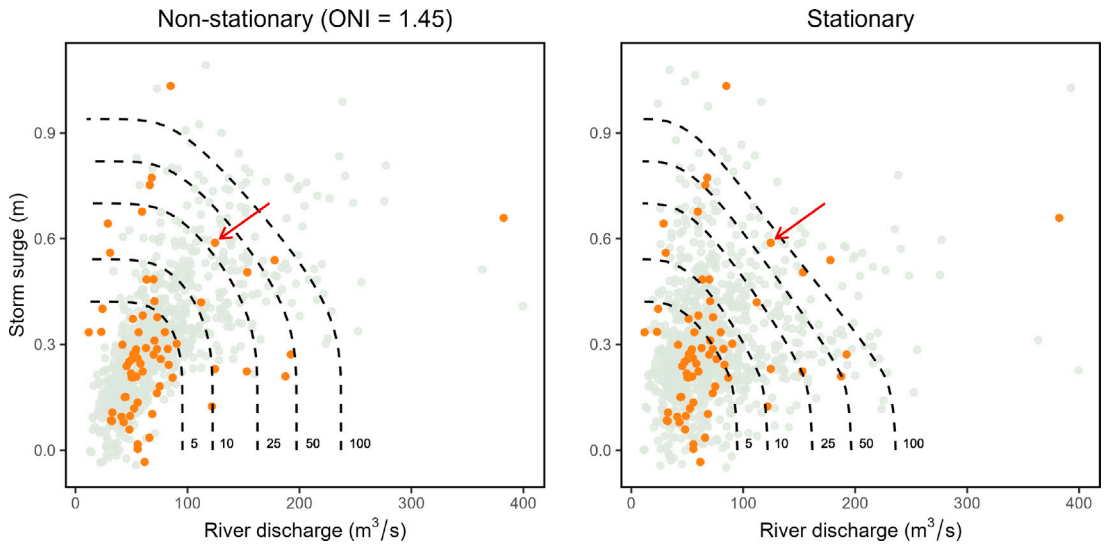


**Fig. 3.** Bivariate hazard curves for Galveston Bay derived from a stationary Frank copula (right) and a dynamic Frank copula for a strong El-Niño year (left). Black dashed lines show the continuous isolines for different return periods ("AND" scenarios), while orange dots represent the observed $Q\_S$ data with the red arrow pointing to an actual compound event of $Q = 125\,\mathrm{m}^3/\mathrm{s}$ and $S = 0.60\,\mathrm{m}$. Dots with light green color illustrate simulations from the bivariate distribution.

be built upon very high-resolution DEM information and incorporate flood protection measures to accurately capture actual compound flood events. The use of spatially continuous global data sets of this kind would also pave the way for including more estuaries, not restricted to US coasts.

Second, the findings presented here are dependent on the covariate used for modeling a dynamic copula, i.e., either ONI or NAO index. In other words, here we have searched for a non-stationary dependence due to ENSO or NAO, only. Even though focusing on these large-scale climate modes is logical from a physics point-of-view for the regions under study, they are non-exhaustive and thus we cannot exclude the possibility that other covariates, which are not used here, might have led to different results with respect to dynamic vs. stationary copula comparison. In simpler terms, for an estuary where we did not detect non-stationarity, the use of a different covariate might have uncovered possibly different and complementary perspectives. Thus, in our future research efforts, we would be interested in evaluating other relevant covariates. For example, we could resort to atmospheric variables like global mean temperature or $CO_2$ concentration, as well as other appropriate climate modes, e.g., Atlantic Multi-decadal Oscillation, which has been shown to affect storm surge in the US Southeast (Park et al., 2011), in order to more comprehensively assess (non-)stationarity.

Finally, another limitation of our work, which however appears difficult to overcome, is the modeling assumption that the copula function itself remains the same over time, but only the magnitude of dependence is changing. In other terms, here we have simplified our analysis, for practical reasons, by hypothesizing that non-stationarity in the dependence structure due to ENSO or NAO, if any, originates with a varying magnitude of dependence and not with a differing copula function. If, for example, a Frank copula was found to provide a good fit for the entire bivariate data set of an estuary, then it was assumed that it provides a good fit for any other subset of that data set. Changing the copula function over time is a rather challenging modeling task and would require very long data records for a statistically robust assessment.

Despite the limitations outlined above, our work constitutes a novel addition to the current scientific literature on dependence between estuarine compound flood drivers. It provides insights about potential non-stationarity due to ENSO and NAO and its implications for bivariate hazard quantification, as well as practical recipes for modeling a stationary/dynamic dependence structure with reduced parametric uncertainty in a Bayesian manner.

## CRediT authorship contribution statement

**Georgios Boumis:** Writing – original draft, Visualization, Software, Methodology, Investigation, Formal analysis, Data curation, Conceptualization. **Hamed R. Moftakhari:** Writing – review & editing, Supervision, Project administration, Funding acquisition, Conceptualization. **Danhyang Lee:** Writing – original draft, Supervision, Methodology. **Hamid Moradkhani:** Writing – review & editing, Project administration, Funding acquisition.

## Declaration of competing interest

The authors declare that they have no known competing financial interests or personal relationships that could have appeared to influence the work reported in this paper.

## Acknowledgments

This study is funded by National Science Foundation, United States awards
#2223893 and #2238000. The authors acknowledge the support of Integrated Research on Disaster Risk (IRDR) Young Scientists Programme (YSP). The first author, Georgios Boumis, is an IRDR Young Scientist (2024–2027).

## Appendix A. Supplementary data

Supplementary material related to this article can be found online at https://doi.org/10.1016/j.advwatres.2024.104858.

## Data availability

Daily river discharge data used in this work can be downloaded from GRDC via: https://grdc.bafg.de/, while hourly coastal water level data can be obtained from GESLA-3 database via: https://gesla787883612.wordpress.com/. The Oceanic Niño Index is accessible through: https://bmcnoldy.earth.miami.edu/tropics/oni/, whereas the North Atlantic Oscillation index can be obtained from: https://climatedataguide.ucar.edu/climate-data/hurrell-north-atlantic-oscillation-nao-index-station-based/. R and Stan scripts as well as data examples that support the analysis presented in this article are freely available and can be accessed via: https://github.com/bgeorgios/BDCop4CF.

## References


Abdi, H., 2007. The Kendall rank correlation coefficient. In: Encyclopedia of Measurement and Statistics, vol. 2, Sage Thousand Oaks, CA, pp. 508–510.

Betancourt, M., 2017. A conceptual introduction to Hamiltonian Monte Carlo. arXiv preprint arXiv:1701.02434.

Boumis, G., Moftakhari, H.R., Moradkhani, H., 2024. A metastatistical frequency analysis of extreme storm surge hazard along the US coastline. Coastal Eng. J. 1–15.

Czado, C., 2019. Analyzing dependent data with vine copulas. In: Lecture Notes in Statistics, Springer, vol. 222, Springer.

Durante, F., Sempi, C., 2010. Copula theory: an introduction. In: Copula Theory and Its Applications: Proceedings of the Workshop. Held in Warsaw, 25-26 September 2009, Springer, pp. 3–31.

Dykstra, S., Dzwonkowski, B., 2021. The role of intensifying precipitation on coastal river flooding and compound river-storm surge events, Northeast Gulf of Mexico. Water Resour. Res. 57 (11), e2020WR029363.

Frees, E.W., Valdez, E.A., 1998. Understanding relationships using copulas. N. Am. Actuar. J. 2 (1), 1–25.

Gelman, A., Hwang, J., Vehtari, A., 2014. Understanding predictive information criteria for Bayesian models. Stat. Comput. 24, 997–1016.

Gelman, A., Lee, D., Guo, J., 2015. Stan: A probabilistic programming language for Bayesian inference and optimization. J. Educ. Behav. Stat. 40 (5), 530–543.

Genest, C., Rémillard, B., Beaudoin, D., 2009. Goodness-of-fit tests for copulas: A review and a power study. Insurance: Math. Econom. 44 (2), 199–213.

Glantz, M.H., Ramirez, I.J., 2020. Reviewing the oceanic Niño index (ONI) to enhance societal readiness for El Niño's impacts. Int. J. Disaster Risk Sci. 11, 394–403.

Gori, A., Lin, N., Xi, D., Emanuel, K., 2022. Tropical cyclone climatology change greatly exacerbates US extreme rainfall–surge hazard. Nature Clim. Change 12 (2), 171–178.

Haigh, I.D., Marcos, M., Talke, S.A., Woodworth, P.L., Hunter, J.R., Hague, B.S., Arns, A., Bradshaw, E., Thompson, P., 2023. GESLA version 3: A major update to the global higher-frequency sea-level dataset. Geosci. Data J. 10 (3), 293–314.

Haigh, I.D., Nicholls, R.J., 2017. Coastal flooding. In: MCCIP Science Review 2017. pp. 98–104.

Harrigan, S., Zsoter, E., Alfieri, L., Prudhomme, C., Salamon, P., Wetterhall, F., Barnard, C., Cloke, H., Pappenberger, F., 2020. GloFAS-ERA5 operational global river discharge reanalysis 1979–present. Earth Syst. Sci. Data 12 (3), 2043–2060.

Harrison, L.M., Coulthard, T.J., Robins, P.E., Lewis, M.J., 2022. Sensitivity of estuaries to compound flooding. Estuaries Coasts 45 (5), 1250–1269.

Hawkes, P.J., Gonzalez-Marco, D., Sánchez-Arcilla, A., Prinos, P., 2008. Best practice for the estimation of extremes: A review. J. Hydraul. Res. 46 (S2), 324–332.

Huang, W., Ye, F., Zhang, Y.J., Park, K., Du, J., Moghimi, S., Myers, E., Pe'eri, S., Calzada, J.R., Yu, H., et al., 2021. Compounding factors for extreme flooding around Galveston Bay during Hurricane Harvey. Ocean Model. 158, 101735.

Hurrell, J.W., Deser, C., 2010. North Atlantic climate variability: the role of the North Atlantic Oscillation. J. Mar. Syst. 79 (3–4), 231–244.

Hurrell, J.W., Kushnir, Y., Ottersen, G., Visbeck, M., 2003. An overview of the North Atlantic oscillation. Geophys. Monogr.-Am. Geophys. Union 134, 1–36.

Jafarzadegan, K., Moradkhani, H., Pappenberger, F., Moftakhari, H., Bates, P., Abbaszadeh, P., Marsooli, R., Ferreira, C., Cloke, H.L., Ogden, F., et al., 2023. Recent advances and new frontiers in riverine and coastal flood modeling. Rev. Geophys. 61 (2), e2022RG000788.

Mentaschi, L., Vousdoukas, M.I., García-Sánchez, G., Fernández-Montblanc, T., Roland, A., Voukouvalas, E., Federico, I., Abdolali, A., Zhang, Y.J., Feyen, L., 2023. A global unstructured, coupled, high-resolution hindcast of waves and storm surge. Front. Mar. Sci. 10, 1233679.

Moftakhari, H.R., Salvadori, G., AghaKouchak, A., Sanders, B.F., Matthew, R.A., 2017. Compounding effects of sea level rise and fluvial flooding. Proc. Natl. Acad. Sci. 114 (37), 9785–9790.

Moftakhari, H., Schubert, J.E., AghaKouchak, A., Matthew, R.A., Sanders, B.F., 2019. Linking statistical and hydrodynamic modeling for compound flood hazard assessment in tidal channels and estuaries. Adv. Water Resour. 128, 28–38.

Nasr, A.A., Wahl, T., Rashid, M.M., Camus, P., Haigh, I.D., 2021. Assessing the dependence structure between oceanographic, fluvial, and pluvial flooding drivers along the United States coastline. Hydrol. Earth Syst. Sci. 25 (12), 6203–6222.

Nasr, A.A., Wahl, T., Rashid, M.M., Jane, R.A., Camus, P., Haigh, I.D., 2023. Temporal changes in dependence between compound coastal and inland flooding drivers around the contiguous United States coastline. Weather Clim. Extrem. 41, 100594.

Park, J., Obeysekera, J., Irizarry, M., Barnes, J., Trimble, P., Park-Said, W., 2011. Storm surge projections and implications for water management in South Florida. Clim. Change 107, 109–128.

Pirani, F.J., Najafi, M.R., 2023. Nonstationary frequency analysis of compound flooding in Canada's coastal zones. Coast. Eng. 182, 104292.

Razmi, A., Mardani-Fard, H.A., Golian, S., Zahmatkesh, Z., 2022. Time-varying univariate and bivariate frequency analysis of nonstationary extreme sea level for New York City. Environ. Process. 9 (1), 8.

Salvadori, G., De Michele, C., 2004. Frequency analysis via copulas: Theoretical aspects and applications to hydrological events. Water Resour. Res. 40 (12).

Salvadori, G., De Michele, C., 2007. On the use of copulas in hydrology: theory and practice. J. Hydrol. Eng. 12 (4), 369–380.

Salvadori, G., De Michele, C., Durante, F., 2011. On the return period and design in a multivariate framework. Hydrol. Earth Syst. Sci. 15 (11), 3293–3305.

Salvadori, G., Durante, F., De Michele, C., Bernardi, M., Petrella, L., 2016. A multivariate copula-based framework for dealing with hazard scenarios and failure probabilities. Water Resour. Res. 52 (5), 3701–3721.

Sebastian, A., 2022. Coastal Flood Risk Reduction. Elsevier, pp. 77–88.

Serafin, K.A., Ruggiero, P., Stockdon, H.F., 2017. The relative contribution of waves, tides, and nontidal residuals to extreme total water levels on US West Coast sandy beaches. Geophys. Res. Lett. 44 (4), 1839–1847.

Sklar, M., 1959. Fonctions de répartition à n dimensions et leurs marges. In: Annales de l'ISUP, Vol. 8, No. 3. pp. 229–231.

Spiegelhalter, D.J., Best, N.G., Carlin, B.P., Van Der Linde, A., 2002. Bayesian measures of model complexity and fit. J. R. Stat. Soc. Ser. B (Stat. Methodol.) 64 (4), 583–639.

Taschetto, A.S., Ummenhofer, C.C., Stuecker, M.F., Dommenget, D., Ashok, K., Rodrigues, R.R., Yeh, S.-W., 2020. El Niño Southern Oscillation in a Changing Climate. Wiley Online Library, pp. 309–335.

Thomas, S., Tu, W., 2021. Learning hamiltonian monte carlo in R. Amer. Statist. 75 (4), 403–413.

Tootoonchi, F., Haerter, J.O., Räty, O., Grabs, T., Sadegh, M., Teutschbein, C., 2020. Copulas for hydroclimatic applications–a practical note on common misconceptions and pitfalls. Hydrol. Earth Syst. Sci. Discuss. 2020, 1–31.

Tootoonchi, F., Sadegh, M., Haerter, J.O., Räty, O., Grabs, T., Teutschbein, C., 2022. Copulas for hydroclimatic analysis: A practice-oriented overview. Wiley Interdiscip. Rev.: Water 9 (2), e1579.

Tripathy, S.S., Jafarzadegan, K., Moftakhari, H., Moradkhani, H., 2024. Dynamic bivariate hazard forecasting of hurricanes for improved disaster preparedness. Commun. Earth Environ. 5 (1), 12.

Valle-Levinson, A., Olabarrieta, M., Heilman, L., 2020. Compound flooding in Houston-Galveston bay during hurricane harvey. Sci. Total Environ. 747, 141272.

Vehtari, A., Gelman, A., Simpson, D., Carpenter, B., Bürkner, P.-C., 2021. Rank-normalization, folding, and localization: An improved $\hat{R}$ for assessing convergence of MCMC (with discussion). Bayesian Anal. 16 (2), 667–718.

Vogl, S., Laux, P., Qiu, W., Mao, G., Kunstmann, H., 2012. Copula-based assimilation of radar and gauge information to derive bias-corrected precipitation fields. Hydrol. Earth Syst. Sci. 16 (7), 2311–2328.

Wahl, T., Jain, S., Bender, J., Meyers, S.D., Luther, M.E., 2015. Increasing risk of compound flooding from storm surge and rainfall for major US cities. Nature Clim. Change 5 (12), 1093–1097.

Wang, H., Xuan, Y., Tran, T.V.T., Couasnon, A., Scussolini, P., Luu, L.N., Nguyen, H.Q., Reeve, D.E., 2023. Changes in seasonal compound floods in Vietnam revealed by a time-varying dependence structure of extreme rainfall and high surge. Coast. Eng. 183, 104330.

Watanabe, S., Opper, M., 2010. Asymptotic equivalence of Bayes cross validation and widely applicable information criterion in singular learning theory. J. Mach. Learn. Res. 11 (12).

Wu, W., Westra, S., Leonard, M., 2021. Estimating the probability of compound floods in estuarine regions. Hydrol. Earth Syst. Sci. 25 (5), 2821–2841.

Zhang, B., Wang, S., Moradkhani, H., Slater, L., Liu, J., 2022. A vine copula-based ensemble projection of precipitation intensity–duration–frequency curves at sub-daily to multi-day time scales. Water Resour. Res. 58 (11), e2022WR032658.